

Auto-generation of a centerline graph from the geometrically complex roadmap of real-world traffic systems using a hierarchical quadtree for cellular automata simulations

Satori Tsuzuki^a, Daichi Yanagisawa^a, Katsuhiro Nishinari^a

^aResearch Center for Advanced Science and Technology, The University of Tokyo, 4-6-1, Komaba, Meguro-ku, Tokyo 153-8904, Japan

Abstract

This paper proposes a method of auto-generation of a centerline graph from the geometrically complex roadmap of real-world traffic systems by using a hierarchical quadtree for cellular automata simulations. Our method is summarized as follows. At first, we store the binary values of the monochrome image of targeting roadmap (one and zero represent the road and the other areas respectively) in the two-dimensional square map. Second, we recursively divide the square map into sub-leaves by a quadtree until each leaf has equal or less than one. Third, we keep removing the distal leaves which adjacent to the leaves whose depth are shallower than the distal leaf, until one step before the distal leaf does not connect to any stable leaves. After that, we trace the remaining distal leaves of the tree using Morton's space-filling curve, while selecting the leaves which keep a certain distance among the previously selected leaves as the nodes of the graph. Finally, each selected node searches the neighboring nodes and stores them as the edges of the graph. We demonstrated our method by generating a centerline graph from a complex roadmap of a real-world airport and by carrying out a typical network analysis using Dijkstra's method.

Keywords: Methodology Study, Graph Generation, Hierarchical Tree Structure, Space-Filling Curves, Cellular Automata

1. INTRODUCTION

A cellular automaton (CA) established by Neumann [1] has attracted scientists and researchers for years. In particular, after Wolfram found the Elementary CA Rule 184 [2], the series of CA have been acknowledged in the field of traffic flow problems. In recent years, the vehicular traffic simulations using CA have taken advantage of the fine-grained background cells to represent the complex geometries of real-world systems. As depicted in Fig. 1, the system selects representative cells on the background cells as the checkpoints and constructs a graph by connecting them. In simulations, the vehicles move on the route of the graph [3, 4, 5, 6, 7]. Each vehicle moves on the centerline of roads in real-world systems. Therefore, the extraction of a centerline graph from a roadmap is an essential process to realize the simulations.

The primary purpose of this research is to propose an effective method to generate a centerline graph from the geometrically complex roadmap of real-world traffic systems. Until today, many studies have reported on the extraction of a centerline graph from the twisted paths in the fields of Computed Tomography [8, 9] and Civil Engineering [10, 11, 12, 13, 14, 15]. However, most of these studies focus on the case that a centerline graph is generated from the boundaries of a roadmap, as shown in the left part of Fig. 2. Conversely, unlike these related studies, we take up a case that we generate a centerline graph from a solid image of a roadmap, as shown in the right part of

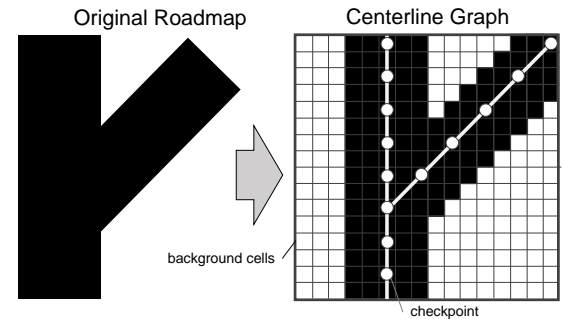


Figure 1: A schematic of the generation of a centerline graph from a roadmap for the traffic simulations using CA.

Fig. 2. Moreover, it is desirable to generate multiple lanes at each intersection of the graph because we aim to use it for the shortest path findings in vehicular traffic systems. Therefore, taking a different approach from existing studies is necessary for the purpose of this study.

In this paper, we propose a method to generate a centerline from the roadmap by dynamically changing the structure of a hierarchical tree, by taking account of the characteristic of the solid images. Our proposed method is summarized as follows. At first, we store the binary values of the monochrome image of targeting roadmap (one and zero represent the road and the other areas respectively) in the two-dimensional square map. Second, we recursively divide the square map into sub-leaves by a quadtree until each leaf has equal or less than one. Third, we gradually remove the distal leaves which adjacent to the leaves whose depth are shallower than the distal leaf, until one step

Email addresses: tsuzuki.satori@mail.u-tokyo.ac.jp (Satori Tsuzuki), tDaichi@mail.ecc.u-tokyo.ac.jp (Daichi Yanagisawa), tknishi@mail.ecc.u-tokyo.ac.jp (Katsuhiro Nishinari)

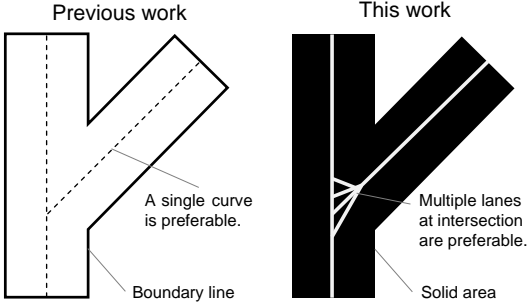


Figure 2: Difference of original roadmap and objectives between previous work and this work.

before the distal leaf does not connect to any stable leaves. After that, we trace the remaining distal leaves of the tree using Morton's space-filling curve [16, 17, 18, 19], while selecting the leaves which keep a certain distance among the previously selected leaves as the nodes of the graph. Finally, each selected node searches the neighboring nodes and stores them as the edges of the graph. In short, we attempt to generate a centerline graph just by releasing distal leaves.

The major characteristics distinguished from the related works are described as follows: 1) the straightforward method using only a hierarchical tree without combining any supportive algorithms such as distance function, 2) the generation from a solid image, and 3) the multiple lanes at each intersection.

In a more broader sense, our method is categorized into the studies of Topological Thinning [20, 21, 22, 23, 24, 25, 26, 27]. Although the concept of shrinking by deleting the boundary cells is same to these studies, our method ensures that we only have to examine the depth of the neighboring leaves, whereas these related studies need the algorithms to preserve the topology of an overall roadmap. Though the study reported in [28] utilizes a quadtree, they use it only to distinguish the internal or external area of a map and to access the cells; each cell judges whether it removes itself or not by referring to the neighboring cells. Therefore, the quadtree needs the reconstruction in every iterative step of the thinning process. To the contrary, our method needs only one-time recursive tree construction during all the procedures; this improves the computational efficiency compared to the previous studies.

The remainder of this paper is structured as follows. Section 2 describes our method in divided four parts. In Section 3, we demonstrate an analysis of the shortest path search by using Dijkstra's algorithm. Section 4 summarizes our results and concludes this paper.

2. METHOD

Figure. 3 shows the targeting roadmap, which we abstracted from the real-world airport, Tokyo International Airport in Japan. We can divide our method into four processes: the construction process of a recursive tree on the roadmap, the release of distal leaves, the selection of nodes, and the connection of nodes by tracing the distal leaves using a space-filling curve, as follows.

2.1. Data structure of leaves

We store each element of the monochrome image of the roadmap depicted in Fig. 3 in a corresponding cell of the two-dimensional $N_r \times N_r$ array. Here, the value of one or zero in each cell represents the road and the other areas, respectively. The parameter N_r denotes the number of cells in either of the vertical or horizontal directions in the original roadmap whichever is a larger size. After that, we recursively divide the square map into 2×2 sub-leaves by a quadtree each leaf of which has the following data structure:

Table. 1: An example of leaf structure.

```
Class Leaf {
    Vector L_min; // Minimum coordinates.
    Vector L_max; // Maximum coordinates.
    int D; // Depth of the leaf.
    int R; // Ordering by parent leaf.
    bool F_end; // Distal leaf or not.
    bool F_del; // To delete (release) or not.
    int S_del; // Sum of F_del.
    bool F_chk; // Checkpoint or not.
    Leaf** child; // Pointer to child leaves.
    Leaf** parent; // Pointer to parent leaf.
}
```

Here, the vector L_{\min} and vector L_{\max} indicates the minimum and maximum coordinates of the leaf and correspond to $(0, 0)$ and (N_r, N_r) at a depth of zero, respectively. The parameter D represents the depth of the leaf. The parameter R indicates the ordering index designated by their parent leaf, which determines the geometric location of the leaf among the bundle of sub-leaves. Here, a space-filling curve is a recursive curve that fills a space or area with a single stroke of a brush [16, 17]. By corresponding the ordering index among sub-leaves to a space-filling curve, it becomes possible to trace all the distal leaves by a single curve. Here, the ordering pattern R is individually determined by the sort of the space-filling curve. We take up Morton's curve (Z-curve) in this paper. The Morton's curve gives indices to sub-leaves in between 0 and 4 so that the trajectory of traversing sub-leaves draw a shape of "Z" character. Therefore, the parameter R always becomes one of the numbers from 0 to 4.

The binary parameter F_{end} represents whether the leaf is a distal leaf or not. We determine the F_{end} of each leaf in Algorithm 1 as described later. Meanwhile, we use the binary parameter F_{del} and parameter S_{del} to judge whether we can release the distal leaf or not in Algorithm 5. In additions, the parameter F_{chk} indicates whether we select the leaf as a node of graph or not and we obtain F_{chk} of each leaf in Algorithm 6.

2.2. Recursive quadtree construction

Algorithm 1 describes the procedure of recursive quadtree construction. The process in line2-9 shows the initialization of all the parameters of the leaf. In the process after line9, we recursively divide the $N_r \times N_r$ map into 2×2 sub-leaves by a quadtree. The parameter B_p indicates the state of a cell, which becomes one when the leaf is inside the road and zero in other cases. At line10, we define B_p^s as the summed up value of B_p

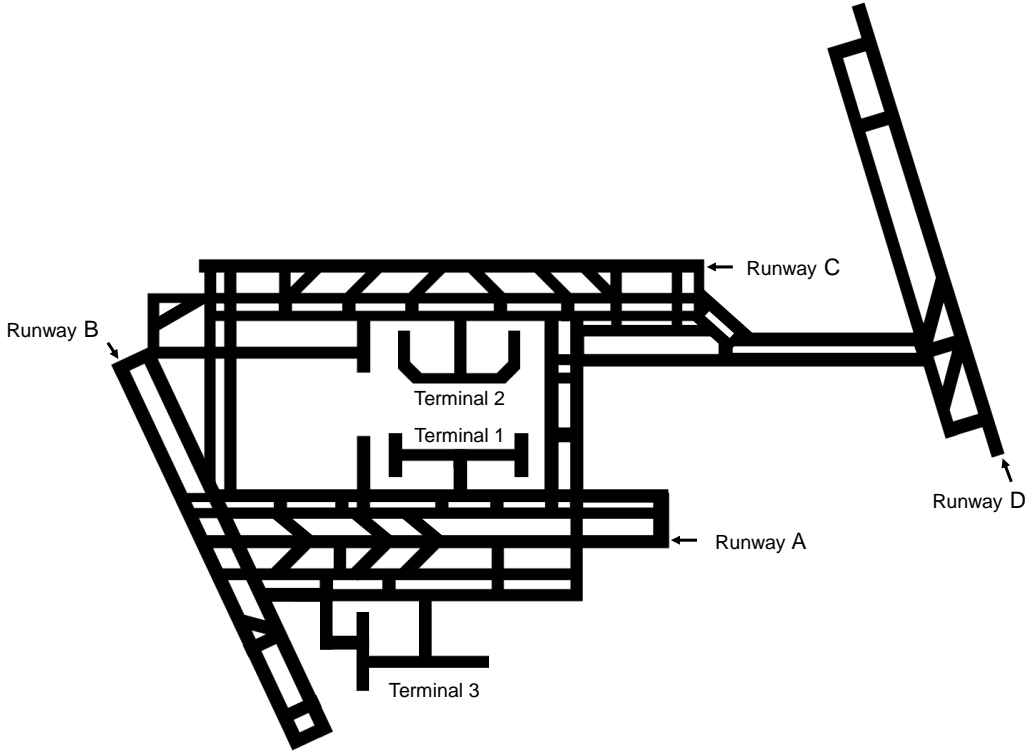


Figure 3: Targeting roadmap abstracted from the real-world airport, Tokyo International Airport in Japan.

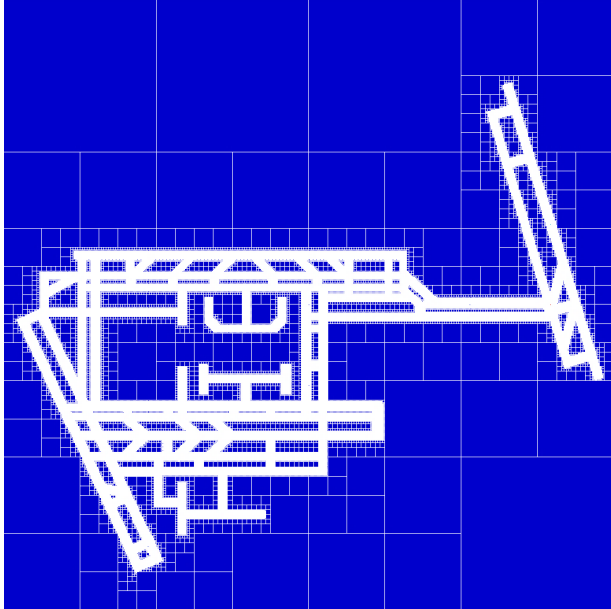


Figure 4: A hierarchically structured mesh constructed on the roadmap in Fig. 3.

inside the leaf. We keep the recursive division of the tree until the value of B_p^s in each leaf becomes equal or less than one. As a result of this, each of the deepest distal leaves respectively corresponds a single cell on the road. Figure 4 shows a hierarchically structured mesh constructed on the roadmap of an airport depicted in Fig. 3. Here, two important observations were made. First, the distal leaves covering the cells on the inner edges of roads always have the maximum depth of the tree. Second, each cell on the inner edges of roads always adjacent to

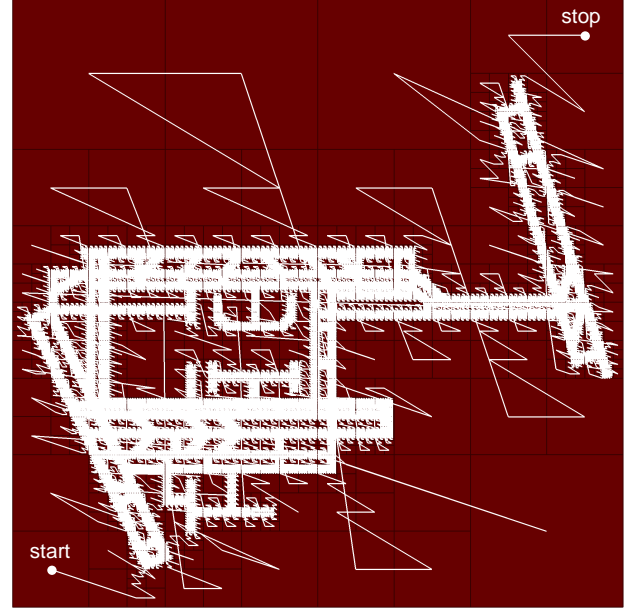


Figure 5: Tracing of all the distal leafs by using Morton's space-filling curve.

other leaves which have a shallower depth than the cell. By utilizing these characteristics, we remain the only leaves located around the center line by releasing leaves through the process from Algorithm 3 to Algorithm 5.

Figure 5 exhibits the process of tracing all the distal leaves by “a single stroke of a brush” using Morton’s curve. Here, for easy access to the distal leaf of the tree, we introduce a conventional technique of a pointer table as shown in Algorithm 2. We can set a sequential number to all the distal leaves by incre-

Algorithm 1 Recursive Tree Construction

```

1: function TREE( $L_{\min}$ ,  $L_{\max}$ ,  $D$ ,  $R$ )
2: Leaf. $L_{\min} \leftarrow L_{\min}$ 
3: Leaf. $L_{\max} \leftarrow L_{\max}$ 
4: Leaf. $D \leftarrow D$ 
5: Leaf. $R \leftarrow R$ 
6: Leaf. $F_{\text{end}} \leftarrow \text{false}$ 
7: Leaf. $F_{\text{del}} \leftarrow \text{false}$ 
8: Leaf. $S_{\text{del}} \leftarrow 0$ 
9: Leaf. $F_{\text{chk}} \leftarrow \text{false}$ 
10: Define  $B_p^s$  as the sum of  $B_p \in [L_{\min}, L_{\max}]$ 
11: if  $B_p^s \leq 1$  then
12:   Leaf. $F_{\text{end}} \leftarrow \text{true}$ 
13:   for  $k = 0, 1 \dots N_{\text{child}} - 1$  do
14:     Leaf.child[k]  $\leftarrow \text{NULL}$ 
15:   end for
16: else
17:   for  $k = 0, 1 \dots N_{\text{child}} - 1$  do
18:     Set  $[L_{\min}^k, L_{\max}^k]$  and  $R^k$  by  $R$ 
19:     Leaf.child[k]  $\leftarrow \text{TREE}(L_{\min}^k, L_{\max}^k, D + 1, R^k)$ 
20:   end for
21: end if
22: return Leaf
23: end function
  
```

menting the number every time Morton's curve traverses two different distal leaves. We can create one more $N_r \times N_r$ array and fill the area paved by a distal leaf with the index of the leaf. Similarly, it is possible to store the pointer of each distal leaf in an $N_r \times N_r$ array, as shown in line8. This pointer table not only makes it easier to access all the distal leaves but also simplifies all the algorithms. Additionally, we store a pointer of the parent leaf at line 2, which we use in the process of release of leaves in Algorithm 5.

Algorithm 2 Generation of Table

```

1: function GENTABLE(Leaf, parent)
2: Leaf.parent  $\leftarrow$  parent
3: if Leaf. $F_{\text{end}} = \text{false}$  then
4:   for  $k = 0, 1 \dots N_{\text{child}} - 1$  do
5:     GENTABLE(Leaf.child[k], Leaf)
6:   end for
7: else
8:   for all  $j$  s.t. Leaf. $L_{\min}.y \leq j \leq L_{\max}.y$  do
9:     for all  $i$  s.t. Leaf. $L_{\min}.x \leq i \leq L_{\max}.x$  do
10:      Table[i][j]  $\leftarrow$  Leaf
11:    end for
12:   end for
13: end if
14: end function
  
```

2.3. Release of distal leaves

Figure 6 illustrates a schematic to release the distal leaves. Here, we take up a one-dimensional case using a binary tree for

easy explanation. The parameter D_{\max}^{mes} indicates the maximum depth of the tree measured by tracing all the distal leaves by Morton's curve. First, we find out the leaves that adjacent to the leaves which have a shallower depth by one level compared to the deepest leaf. We set flags to them as the candidates and change the F_{del} of them from false to true. In this example case, we set the flags to the leaf d and leaf f as the candidates because the leaf e has a shallower depth. We need to prevent the tree from the over-release of leaves because the tree releases them by a unit of a bundle of sub-leaves. We count the number of F_{del} whose state is true in every bundle of sub-leaves and store it to the S_{del} of their parent leaf. In case that a leaf has the S_{del} whose value is zero, the leaf has no candidate sub-leaf to be released. Hereafter, we name such a leaf as "a stable leaf." Next, the leaf B searches the state of neighboring leaves (A and C). Because leaf B is connected with a stable leaf A , we keep the distal leaf d as a candidate sub-leaf to be released. On the other hand, we have to exclude the leaf f from the list of candidates regardless of the state of the leaf D because the leaf f connects with a vacant leaf g which locates outside the roads. In the end, the leaf B , a bundle comprising the leaf c and leaf d , is released.

Algorithm 3 Selection of Candidates

```

1: function SELECTCANDIDATE(Leaf)
2: if Leaf. $F_{\text{end}} = \text{false}$  then
3:   for  $k = 0, 1 \dots N_{\text{child}} - 1$  do
4:     SELECTCANDIDATE(Leaf.child[k])
5:   end for
6: else
7:   if Leaf. $D = D_{\max}^{\text{mes}}$  then
8:     flag  $\leftarrow \text{false}$ 
9:     i  $\leftarrow$  Leaf. $L_{\min}.x$ 
10:    j  $\leftarrow$  Leaf. $L_{\min}.y$ 
11:    d  $\leftarrow$  (Table[i+1][j].D)
12:    if d  $< D_{\max}^{\text{mes}}$  then
13:      flag  $\leftarrow \text{true}$ 
14:    end if
15:    d  $\leftarrow$  (Table[i-1][j].D)
16:    if d  $< D_{\max}^{\text{mes}}$  then
17:      flag  $\leftarrow \text{true}$ 
18:    end if
19:    d  $\leftarrow$  (Table[i][j+1].D)
20:    if d  $< D_{\max}^{\text{mes}}$  then
21:      flag  $\leftarrow \text{true}$ 
22:    end if
23:    d  $\leftarrow$  (Table[i][j-1].D)
24:    if d  $< D_{\max}^{\text{mes}}$  then
25:      flag  $\leftarrow \text{true}$ 
26:    end if
27:    if flag = true then
28:      Leaf. $F_{\text{del}} \leftarrow \text{true}$ 
29:    end if
30:  end if
31: end if
32: end function
  
```

Algorithm 3 shows the procedure of selecting the candidates

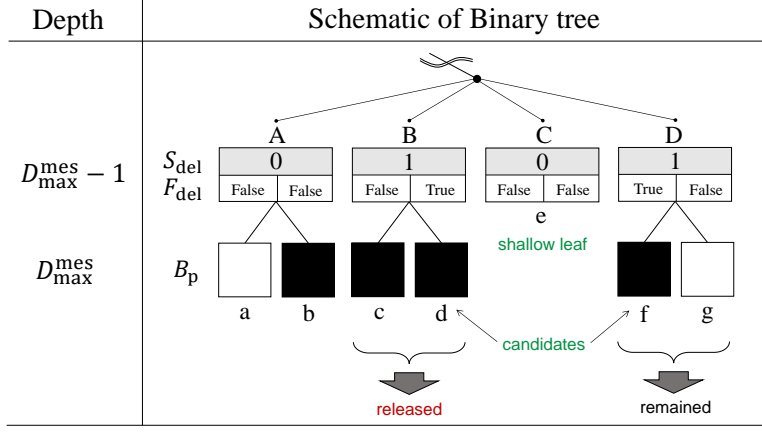


Figure 6: A schematic explanation to release the distal leaves.

Algorithm 4 Sum of F_{del} over a Bundle of Sub-leaves

```

1: function CHECKBRANCHES(Leaf)
2:   if Leaf.D  $\neq D_{\max}$  and
3:     Leaf.D  $\neq D_{\max} - 1$  then
4:       for k = 0,1... $N_{\text{child}} - 1$  do
5:         CHECKBRANCHES(Leaf.child[k])
6:       end for
7:     else
8:       if Leaf.D =  $D_{\max} - 1$  then
9:         Leaf.Sdel  $\leftarrow 0$ 
10:        for k = 0,1... $N_{\text{child}} - 1$  do
11:          if Leaf.child[k]. $F_{\text{del}}$  = true then
12:            Leaf.Sdel  $\leftarrow$  Leaf.Sdel + 1
13:          end if
14:        end for
15:      end if
16:    end if
17:  end function

```

to be released. First, we detect one of the distal leaves by the process in line 2-6. After finding a distal leaf, we examine the depth of the neighboring four leaves existing in the vertical or horizontal direction of the distal leaf as described in line12-26. If we find that at least one of four neighboring leaves has a shallower depth than D_{\max} , we change the F_{del} of the leaf from false to true as in line27-29. After that, in Algorithm 4, we count the number of F_{del} whose state is true in every bundle of sub-leaves and store it to S_{del} of their parent leaf as described in line 9-14. As aforementioned, when the value of S_{del} of a leaf becomes zero, the leaf has no candidate sub-leaf to be released (the leaf can be said as “stable leaf”).

Finally, we remove leaves according to the procedure in Algorithm 5. We detect one of the parents of distal leaves by the process in line2-7. After finding a parent of a distal leaf, we descend to each of four child leaves of the leaf as described in line10. We examine the value of S_{del} of each parent of the leaves which neighbors to each child leaf as described in line13-24. When the value of S_{del} becomes zero, a bundle of the leaves including the neighboring leaf of the child leaf remains; we conclude that the child leaf is connected to “a stable leaf”. In this

case, we change the F_{nbr} from false to true. On the other hand, we check the value of F_{del} of each child leaf. In the case at least one of F_{del} of child leaves is true, we change F_{cnd} from false to true in line27-32. As long as both F_{nbr} and F_{cnd} are true, we release all the child leaves as described in line33-39.

We set the parameter F_{stop} to be false at the root of the tree. By examining the value of F_{stop} after conducting the Algorithm 5, we can judge whether the release of leaves occurs at least once or not. We repeat the procedures from Algorithm 3 to Algorithm 5 to shrink the area around the centerline. Noted that it is necessary to update the pointer table Table(i,j) and D_{\max} at every step after executing the process from Algorithm 3 to Algorithm 5.

Let us define N_{rep} as the number of repeating the shrinking process and define N_{rep}^{\max} as the number of repeating that until F_{stop} changes false to true. Practically, repeating N_{rep}^{\max} times of the shrinking process often causes the over-release of leaves. In an example case shown in Fig. 7, the parameter N_{rep}^{\max} becomes eighteen while it is adequate to set N_{rep} to be six for generating a centerline graph. Hence, it is reasonable to regard the parameter N_{rep}^{\max} as a limit of iteration; at present, the actual number of N_{rep} needs adjusting in individual cases in the range from zero to N_{rep}^{\max} .

2.4. Selection and connection of nodes

After shrinking the road areas by Algorithm 5, we trace all the remaining distal leaves of the tree by Morton’s curve to choose the nodes from these distal leaves which keep a certain distance among the previously selected nodes as described in Algorithm 6. To begin with, we detect one of the distal leaves by the procedure in line2-6. After finding a distal leaf, we check the distance between the leaf and all the already registered nodes in line8-14. Here, the parameter $N_{\text{chk}}^{\text{crr}}$ represents the number of registered nodes. In case that all the distances between the leaf and each node registered at that time become larger than a certain distance η , we change the F_{chk} of the leaf from false to true and add the leaf to the list of registered nodes. After that, we increment the parameter $N_{\text{chk}}^{\text{crr}}$ by one as shown in line18.

Algorithm 7 describes a procedure of connection of nodes and Figure 8 gives a schematic explanation of it. At first, we

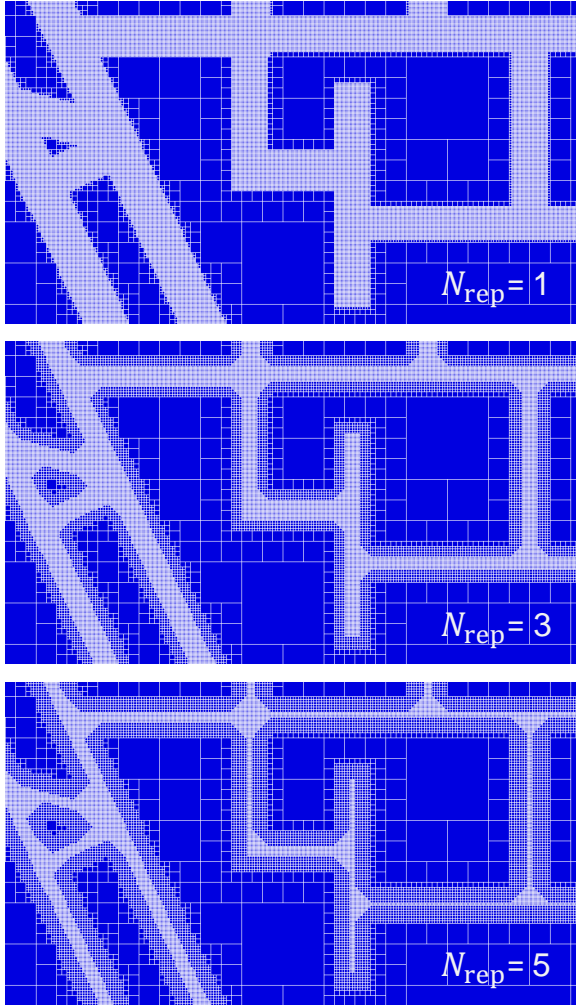


Figure 7: A shrinking process of areas around the centerline for different values of parameter N_{rep} between 1 and 5.

define a cut-off radius of ϵ . Each node searches the other nodes which locate within the range ϵ as in line5-6 of Algorithm 7. When the node j find that another node i satisfies this condition, the node j checks whether the relative vector from node j to node i only traverses the cells on roads as in line7-18. If it is true, the node j add the node i to its connectivity list as shown in line19-21.

The cut-off radius ϵ is the parameter that controls the degree of the connectivities among the nodes; we experimentally determine it within a few times as large as the parameter η in typical to strengthen the connectivity at intersections while keeping the geometry of the original roadmap. To summarize, we have two deterministic parameters and two experimental parameters: the number of cells in one direction N_r , the distance among nodes η , the number of repeating the shrinking process N_{rep} , and the cut-off radius ϵ .

Figure 9 shows a generated graph from the roadmap of Fig. 1 by the procedures using from Algorithm 1 to Algorithm 7 and Figure 10 exhibits an enlarged view of Fig. 9. The white-colored rectangle lines indicate the hierarchically structured

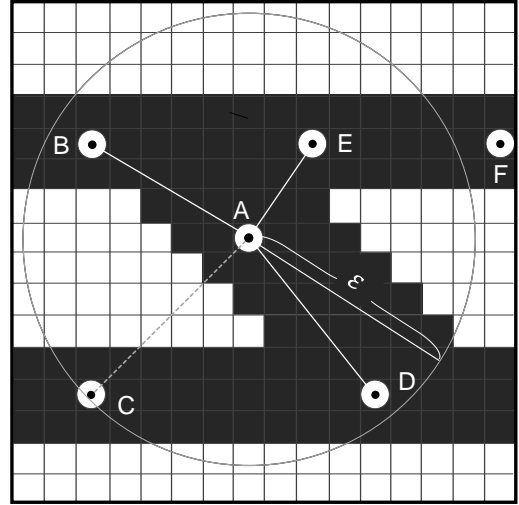


Figure 8: Schematic view of connecting nodes.

leaves at a depth of zero, for reference. We set the pair of $(N_r, \eta, N_{\text{rep}}, \epsilon)$ to be $(2048, 8, 8, 28)$ to generate the graph. It was confirmed that the paths were constructed near the centerlines at the straight roads and multiple lanes were connected at around each intersection.

3. GRAPH NETWORK ANALYSIS

3.1. A short path search using Dijkstra's algorithm

To demonstrate the effectiveness of our method, we carry out a shortest-path finding using Dijkstra's Algorithm for a network generated from Tokyo International Airport in Japan. In one example, we calculate the shortest paths from the entrance of high-speed taxiway in runway B to the departure lane of runway C or that of runway D via a checkpoint in Terminal 1. Figure 11 shows the calculated paths from the node a to node b or node c via node d by using Dijkstra's algorithm, and Figure 12 exhibits an enlarged view of Figure 11. Several reasonable results are observed. First, the calculated paths show a characteristic of Euclidean distance rather than Manhattan distance because of the high-resolution image of the roadmap. We confirmed that the path connecting the node a and node d crosses the runway A diagonally as much as possible. This is understandable because of a relation of “triangle inequality” among three edges of a rectangle the diagonal vertices of which are given as the node a and node b . The similar explanation can be made to the fact that the path connecting the node d and node c shows two straight lanes including a single corner.

4. CONCLUSIONS

In this paper, we proposed an effective method of auto-generation of a centerline graph from the geometrically complex roadmap of real-world traffic systems by using a hierarchically structured tree.

Our method is summarized as follows. At first, we store the binary values of a solid image of a roadmap in the two-dimensional square map. Second, we recursively divide the square map into sub-leaves by a quadtree until each leaf has equal or less than one. Third, we gradually remove the distal leaves which adjacent to the leaves whose depth are shallower than the distal leaf, until one step before the distal leaf does not connect to any stable leaves. After that, we trace the remaining distal leaves of the tree using Morton's curve, while selecting the leaves which keep a certain distance among the previously selected leaves as the nodes of the graph. In the end, each selected node searches the neighboring nodes and stores them as the edges of the graph.

Our method has following notable features: 1) the straightforward method using only a hierarchical tree without combining any other supportive algorithms such as distance function, 2) the generation from a solid image, and 3) the multiple lanes at each intersection. Besides, our method ensures that we can generate a graph without executing the algorithms to preserve the topography of an overall roadmap; this is an emphasizing point compared to the related works. Additionally, we demonstrated a shortest-path finding of the generated graph using Dijkstra's algorithm. It is quite meaningful that we successfully developed a new technology to generate the network graph that is suitable for the studies of vehicular traffic simulations in transportation researches.

Acknowledgements

This research was supported by MEXT as “Post-K Computer Exploratory Challenges” (Exploratory Challenge 2: Construction of Models for Interaction Among Multiple Socioeconomic Phenomena, Model Development and its Applications for Enabling Robust and Optimized Social Transportation Systems)(Project ID: hp190163), partly supported by JSPS KAKENHI Grant Numbers 25287026, 15K17583 and 18H06459.

References

- [1] J. V. Neumann, *Theory of Self-Reproducing Automata* (University of Illinois Press, Champaign, IL, USA, 1966).
- [2] S. Wolfram, Statistical Mechanics of Cellular Automata, *Rev. Mod. Phys.* **55**, 601 (1983).
- [3] K. Yamamoto, S. Kokubo, and K. Nishinari, Simulation for Pedestrian Dynamics by Real-Coded Cellular Automata (rca), *Physica A: Statistical Mechanics and its Applications* **379**, 654 (2007).
- [4] F. Mazur and M. Schreckenberg, Simulation and Optimization of Ground Traffic on Airports using Cellular Automata, *Collective Dynamics* **3**, 1 (2018).
- [5] S. Tsuzuki, D. Yanagisawa, and K. Nishinari, Throughput reduction on the air-ground transport system by the simultaneous effect of multiple traveling routes equipped with parking sites, 2019, arXiv:1901.10390.
- [6] R. Mori, Aircraft Ground-Taxiing Model for Congested Airport Using Cellular Automata, *IEEE Trans. Intelligent Transport. Sys* **14**, 180 (2013).
- [7] C. Feliciani and K. Nishinari, An improved cellular automata model to simulate the behavior of high density crowd and validation by experimental data, *Physica A: Statistical Mechanics and its Applications* **451**, 135 (2016).
- [8] I. Bitter and A. Kaufman, Automatic centerline extraction for virtual colonoscopy, *IEEE Transactions on Medical Imaging* **21**, 1450 (2002).
- [9] M. Wei *et al.*, Centerline extraction of vasculature mesh, *IEEE Access* **6**, 10257 (2018).
- [10] J.-H. Haunert and M. Sester, Area collapse and road centerlines based on straight skeletons, *GeoInformatica* **12**, 169 (2008).
- [11] P. Yuqing, C. Wencho, and S. Yehua, The shortest hypotenuse-based centerline generation algorithm, 2009.
- [12] C. Cao and Y. Sun, Automatic road centerline extraction from imagery using road gps data, *Remote Sensing* **6**, 9014 (2014).
- [13] M. McAllister and J. Snoeyink, Medial axis generalization of river networks, *Cartography and Geographic Information Science* **27**, 129 (2000), <https://doi.org/10.1559/152304000783547966>.
- [14] Y. Zhong and F. Chen, Computing medial axis transformations of 2d point clouds, *Graphical Models* **97**, 50 (2018).
- [15] Q. Li, H. Fan, X. Luan, B. Yang, and L. Liu, Polygon-based approach for extracting multilane roads from openstreetmap urban road networks, *International Journal of Geographical Information Science* **28**, 2200 (2014), <https://doi.org/10.1080/13658816.2014.915401>.
- [16] C. Konrad, INRIA Report No. RR-6693, 2008 (unpublished).
- [17] S. Aluru and F. Sevilgen, Parallel domain decomposition and load balancing using space-filling curves, in *High-Performance Computing, 1997. Proceedings. Fourth International Conference on*, pp. 230–235, 1997.
- [18] S. Tsuzuki and T. Aoki, Effective dynamic load balance using space-filling curves for large-scale sph simulations on gpu-rich supercomputers, in *Proceedings of the 7th Workshop on Latest Advances in Scalable Algorithms for Large-Scale Systems, ScalA '16*, pp. 1–8, Piscataway, NJ, USA, 2016, IEEE Press.
- [19] C. Muelder and K. Ma, Rapid graph layout using space filling curves, *IEEE Transactions on Visualization and Computer Graphics* **14**, 1301 (2008).
- [20] Y. K. Chu and C. Y. Suen, An alternate smoothing and stripping algorithm for thinning digital binary patterns, *Signal Processing* **11**, 207 (1986).
- [21] C. Ronse, A topological characterization of thinning, *Theoretical Computer Science* **43**, 31 (1986).
- [22] C. Ma, On topology preservation in 3d thinning, *CVGIP: Image Understanding* **59**, 328 (1994).
- [23] G. Németh, P. Kardos, and K. Palágyi, 2d parallel thinning and shrinking based on sufficient conditions for topology preservation, *Acta Cybernetica* **20**, 125 (2011).
- [24] N. Passat, M. Couprise, L. Mazo, and G. Bertrand, Topological properties of thinning in 2-d pseudomanifolds, *J. Math. Imaging Vis.* **37**, 27 (2010).
- [25] G. Nmeth and K. Palgyi, Topology preserving parallel thinning algorithms, *International Journal of Imaging Systems and Technology* **21**, 37, <https://onlinelibrary.wiley.com/doi/pdf/10.1002/ima.20272>.
- [26] K. Palgyi, J. Tschirren, E. A. Hoffman, and M. Sonka, Quantitative analysis of pulmonary airway tree structures, *Computers in Biology and Medicine* **36**, 974 (2006).
- [27] S. S. Abeysinghe and T. Ju, Interactive skeletonization of intensity volumes, *The Visual Computer* **25**, 627 (2009).
- [28] W.-T. Wong, F. Y. Shih, and T.-F. Su, Thinning algorithms based on quadtree and octree representations, *Information Sciences* **176**, 1379 (2006).

Algorithm 5 Release of leaves

```

1: function RELEASELEAVES(Leaf,  $F_{stop}$ )
2:   if Leaf.D  $\neq D_{max}^{mes}$  and
3:     Leaf.D  $\neq D_{max}^{mes} - 1$  then
4:       for k = 0,1... $N_{child} - 1$  do
5:         RELEASELEAVES(Leaf.child[k],  $F_{stop}$ )
6:       end for
7:     else
8:       if Leaf.D =  $D_{max}^{mes} - 1$  then
9:          $F_{nbr} \leftarrow$  false
10:        for k = 0,1... $N_{child} - 1$  do
11:          i  $\leftarrow$  Leaf.child[k]. $L_{min.x}$ 
12:          j  $\leftarrow$  Leaf.child[k]. $L_{min.y}$ 
13:          for all J s.t.  $j - 1 \leq J \leq j + 1$  do
14:            for all I s.t.  $i - 1 \leq I \leq i + 1$  do
15:              if (i,j)  $\neq$  (I,J) then
16:                d  $\leftarrow$  Table[I][J].D
17:                if d =  $D_{max}^{mes}$  then
18:                  s  $\leftarrow$  Table[I][J].parent. $S_{del}$ 
19:                  if s = 0 then
20:                     $F_{nbr} \leftarrow$  true
21:                  end if
22:                end if
23:              end if
24:            end for
25:          end for
26:        end for
27:         $F_{cnd} \leftarrow$  false
28:        for k = 0,1... $N_{child} - 1$  do
29:          if Leaf.child[k]. $F_{del}$  = true then
30:             $F_{cnd} \leftarrow$  true
31:          end if
32:        end for
33:        if  $F_{nbr}$  = true and  $F_{cnd}$  = true then
34:          Leaf. $F_{end} \leftarrow$  true
35:          for k = 0,1... $N_{child} - 1$  do
36:            delete Leaf.child[k]
37:             $F_{stop} \leftarrow$  true
38:          end for
39:        end if
40:      end if
41:    end if
42:  end function
  
```

Algorithm 6 Selection of Nodes

```

1: function SELECTNODES(Leaf)
2:   if Leaf. $F_{end}$  = false then
3:     for k = 0,1... $N_{child} - 1$  do
4:       SELECTNODES(Leaf.child[k])
5:     end for
6:   else
7:     if Leaf.D =  $D_{max}^{mes}$  then
8:       F  $\leftarrow$  true
9:       for j = 0,1... $N_{chk}^{crr} - 1$  do
10:        d = DISTANCE(node[j].pos, Leaf.pos)
11:        if d <  $\eta$  then
12:          F  $\leftarrow$  false
13:        end if
14:      end for
15:      if F = true then
16:        Leaf. $F_{chk} \leftarrow$  true
17:        add Leaf to the list of nodes
18:         $N_{chk}^{crr} \leftarrow N_{chk}^{crr} + 1$ 
19:      end if
20:    end if
21:  end if
22: end function
  
```

Algorithm 7 Connection of selected nodes

```

1: for j = 0,1... $N_{node} - 1$  do
2:   node[j].list  $\leftarrow$  null
3:   for i = 0,1... $N_{node} - 1$  do
4:     if i  $\neq$  j then
5:       d = DISTANCE(node[j].pos, node[i].pos)
6:       if d <  $\epsilon$  then
7:         define A as a relative vector from j to i
8:         define n as a unit vector of A
9:         k  $\leftarrow$  0
10:        pos  $\leftarrow$  node[j].pos
11:        flag  $\leftarrow$  true
12:        while pos  $\neq$  node[i].pos do
13:          pos  $\leftarrow$  pos + kn
14:          if  $B_p$  at pos = 0 then
15:            flag  $\leftarrow$  false
16:          end if
17:          k  $\leftarrow$  k+1
18:        end while
19:        if flag = true then
20:          add node[i] to node[j].list
21:        end if
22:      end if
23:    end if
24:  end for
25: end for
  
```

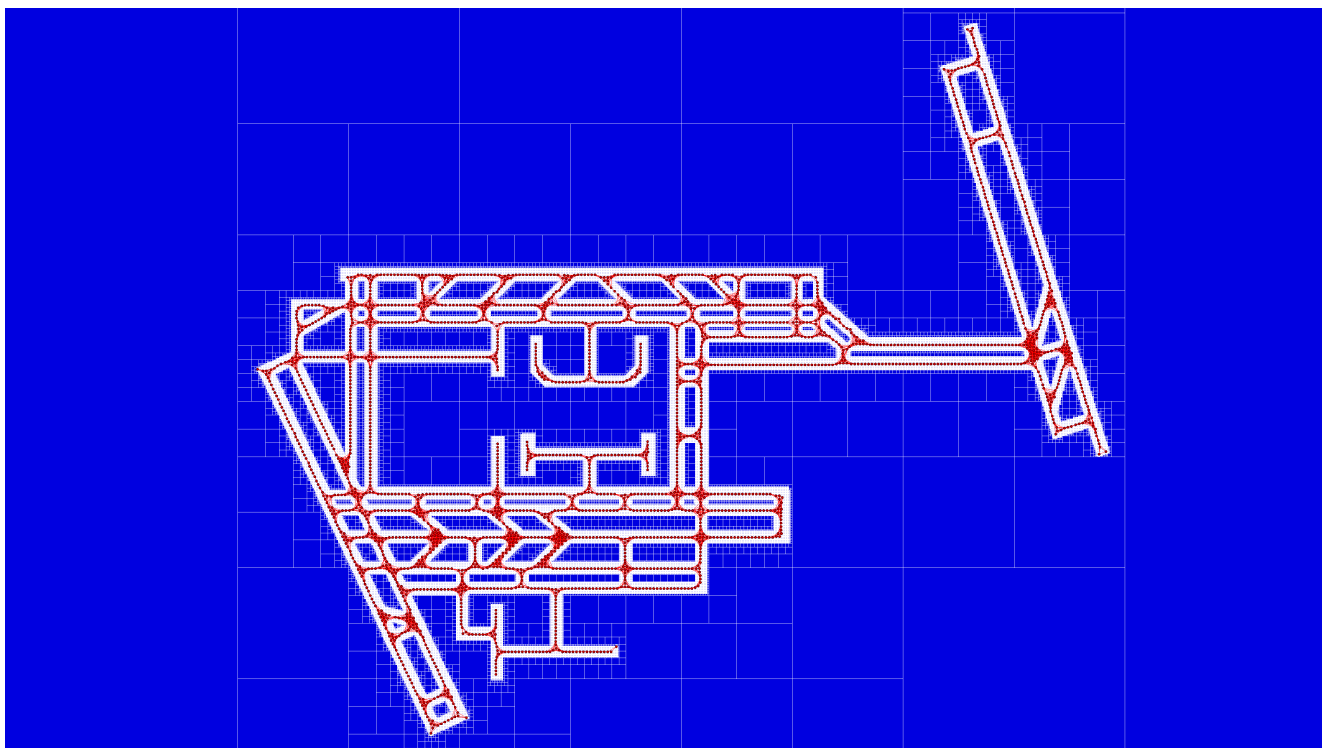


Figure 9: A generated graph from the roadmap of Fig. 1 by the procedures using from Algorithm 1 to Algorithm 7.

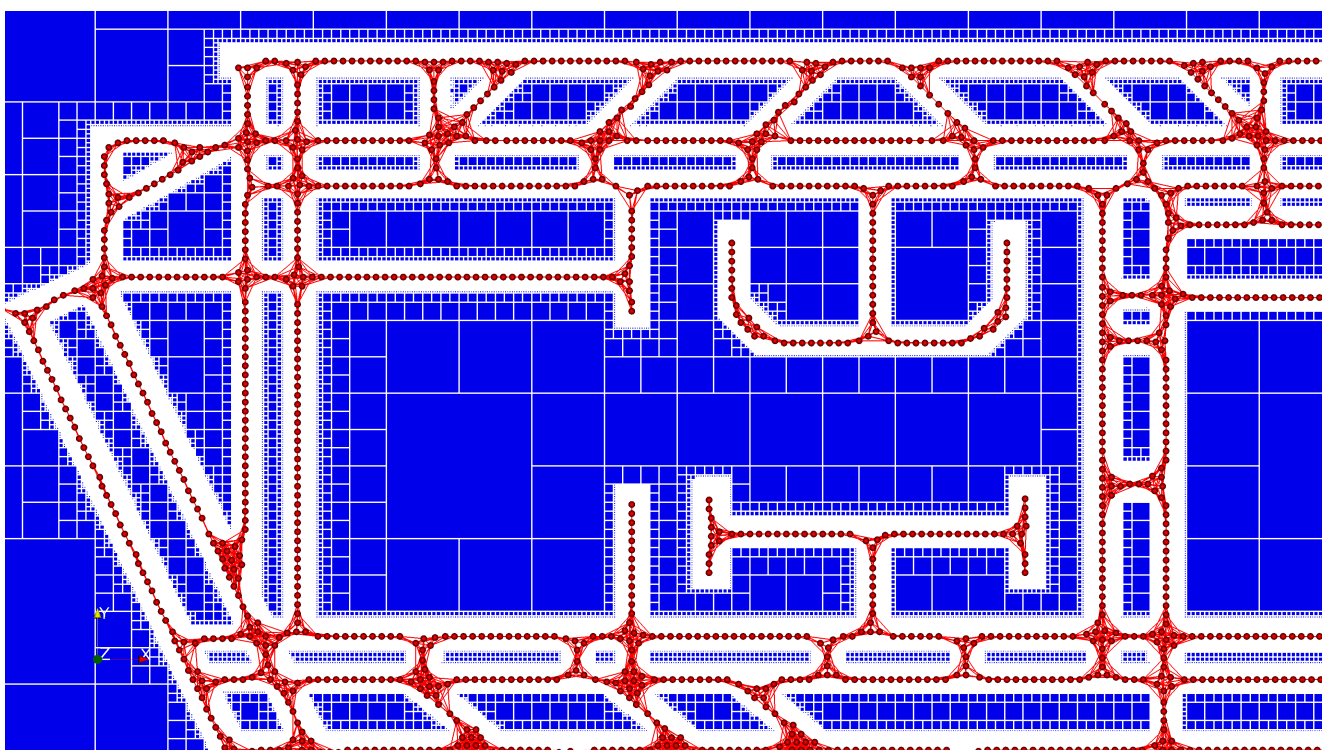


Figure 10: An enlarged view of Fig.9.

